

## Resonant level formed by tin in $\text{Bi}_2\text{Te}_3$ and the enhancement of room-temperature thermoelectric power

Christopher M. Jaworski

*Department of Mechanical Engineering, Ohio State University, Columbus, Ohio 43210, USA*

Vladimir Kulbachinskii

*Low Temperature Physics Department, Physics Faculty, Moscow State University, 119991 GSP-1 Moscow, Russia*

Joseph P. Heremans

*Department of Mechanical Engineering and Department of Physics, Ohio State University, Columbus, Ohio 43210, USA*

(Received 1 June 2009; revised manuscript received 24 October 2009; published 16 December 2009)

Tin is a known resonant impurity in the valence band of  $\text{Bi}_2\text{Te}_3$  that was previously reported to enhance the thermoelectric power  $S$  of the host material at cryogenic temperatures through resonant scattering. We show here that Sn provides an excess density of states (DOS) about 15 meV below the valence band edge and that it is the increases in DOS itself that enhances  $S$  of this technologically important semiconductor even at room temperature. The experimental proof for the existence of this resonant level comes from Shubnikov-de Haas measurements combined with galvanomagnetic and thermomagnetic properties measurements.

DOI: [10.1103/PhysRevB.80.233201](https://doi.org/10.1103/PhysRevB.80.233201)

PACS number(s): 84.60.Rb, 71.20.Nr, 71.55.Ht

The distortion of the density of states by a resonant impurity was shown recently<sup>1</sup> to double the thermoelectric figure of merit  $zT$  of the parent semiconductor in the case of thallium-doped PbTe. The concept of an impurity-induced resonant state, also known as a “virtual bound state,” was introduced by Friedel<sup>2</sup> as a bound state with a positive energy with respect to the band edge, i.e. with the same energy as an extended state. If it can resonate with a component of that extended state, it builds up two extended states of slightly different energies; these in turn have the same energies as the extended states with whom they will resonate, and so on, until an excess density of states arises over a narrow energy range in the band of the host material. Soon after their discovery, virtual bound states in metals were shown to lead to an increase in thermoelectric power of the host metal by a mechanism now known as resonant scattering;<sup>3</sup> this evolved into the Kondo<sup>4</sup> theory when applied to dilute alloys of magnetic impurities in metals. Resonant levels<sup>5</sup> and resonant scattering<sup>6</sup> were also observed in semiconductors such as PbTe. Even if some metals can have Kondo temperatures in excess of 300 K, acoustic and optical phonon scattering far exceeds resonant scattering at all but cryogenic temperatures in most metals and in all semiconductors: Ravich<sup>6</sup> recognizes that resonant scattering is not a practical mechanism for enhancing the thermoelectric properties of semiconductors above the cryogenic range. Contrasting with the resonant scattering concept, Mahan and Sofo<sup>7</sup> suggest that the thermopower and the thermoelectric figure of merit can be boosted intrinsically by the excess density of states itself. Because this mechanism does not involve any scattering, it is in essence temperature independent (except for the temperature dependence of the band structure itself),<sup>8</sup> and thus suitable for enhancing the figure of merit in practical thermoelectric materials at and above room temperature. It is this mechanism that was shown to be at work in high- $zT$  PbTe:TI.<sup>1</sup> In this Brief Report, we identify tin as a resonant level capable of a similar enhancement at room temperature in the classical thermoelectric semiconductor,  $\text{Bi}_2\text{Te}_3$ , which is the parent material for alloys widely used in Peltier cool-

ing. Experimental proof of this realization, however, is complicated by the lower valence band that is located much closer in energy to the upper valence band than that of PbTe.

$\text{Bi}_2\text{Te}_3$ 's upper valence bands (UVBs) have Fermi surfaces that consist of six ellipsoidal pockets in  $\mathbf{k}$  space,<sup>9</sup> centered in the mirror plane of the Brillouin zone lying along  $(0.3-0.5) |\Gamma X|$  (Ref. 10) direction, and have an integral density of states (DOS) effective mass  $m_d^* = 0.35m_e$ .<sup>10</sup> A lower, heavier valence band (LVB), consisting of six ellipsoids, has been shown to exist 20.5 meV below the UVB in  $\mathbf{k}$  space at  $(0.3-0.4) |\Gamma A|$ .<sup>9</sup>  $\text{Bi}_2\text{Te}_3$  can be doped  $p$  type with extrinsic atoms such as Ge, Sn, Pb, or  $n$  type with In, Cl, or I. It is known that tin forms a resonant state 15 meV (Refs. 11 and 12) below the top of the UVB at 2 K and “stabilizes” the Seebeck coefficient  $S$  of single crystals of  $\text{Bi}_2\text{Te}_3$ .<sup>13</sup> The inset in Fig. 1 illustrates the suggested energy level layout. Zhitinskaya<sup>14,15</sup> indeed reported an enhancement of the thermopower at a given hole concentration near liquid nitrogen temperature, but ascribed it to resonant scattering, which suggested that this effect would be limited to low temperatures.<sup>16</sup>

Here we report thermomagnetic transport properties and Shubnikov–de Haas (SdH) data, and conclude that Sn is a

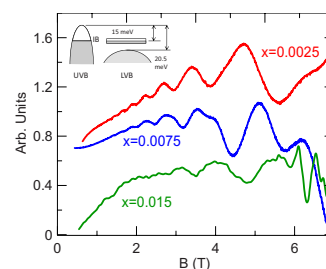


FIG. 1. (Color online) SdH traces for samples studied here. The inset contains the proposed valence band energy layout. The amplitude of the SdH oscillations first increase with  $x$  from  $x=0.0025$  to  $0.0075$  and then decrease again for  $x=0.015$ ; this is discussed in Ref. 30. The trace for  $x=0.015$  has been magnified by  $10^5$ , and the background subtracted.

resonant impurity that distorts the valence band dispersion of  $\text{Bi}_2\text{Te}_3$  and strongly enhances its thermoelectric power at room temperature.

Tin-doped bismuth telluride ( $\text{Bi}_{2-x}\text{Sn}_x\text{Te}_3$ ) with nominal concentrations in the melt of  $x=0.0025$ ,  $0.0075$ , and  $0.015$  single crystals were grown using a modified Bridgeman technique; these were used for both thermoelectric and Shubnikov-de Haas measurements. We grew three additional single crystals (one with  $x=0.02$ , and two with  $x=0.05$ ) used only for the thermoelectric measurements, which were heated to  $700^\circ\text{C}$ , rocked, cooled to  $600^\circ\text{C}$  and then pulled in a Bridgeman apparatus. We will see that the thermoelectric properties correlate more with the Hall data than with the actual amount of Sn put in the melt. The samples' long axis (index 1) were in the plane perpendicular to the  $\langle 001 \rangle$  direction. We measure SdH oscillations in both resistivity and Hall coefficient at  $1.9\text{ K}$  with the magnetic field oriented along the trigonal direction  $H_3 \parallel \langle 001 \rangle$  and swept from  $-7\text{ T}$  to  $7\text{ T}$ , and deduce the cross-sectional areas of the Fermi surfaces. We also report four thermomagnetic and galvanomagnetic coefficients measured as in Ref. 17. The isothermal transverse Nernst-Ettingshausen coefficient  $N[=N_{21}(H_3)]$ , was measured from  $77\text{--}400\text{ K}$  while Hall coefficient  $R_H[=R_{H21}(H_3)]$ , thermopower  $S(=S_{11})$ , and resistivity  $\rho(=\rho_{11})$  were measured from  $2\text{--}400\text{ K}$ . From these measurements, we calculate the Fermi level, carrier mobility, effective mass, and scattering exponent at each temperature.<sup>18</sup> The main source of error on the measurements of Seebeck coefficient is related to the difficulty in measuring voltage and temperature at precisely the same location. We use copper/constantan thermocouples welded to the sample to measure temperatures, and the same Cu wires to measure the voltage; care is taken to minimize the size of the contact and to use wire of  $25\ \mu\text{m}$  diameter to limit its heat draining capability. We estimate the error on  $S_{11}$  on the order of 3%. The major source of errors on measurements of  $N_{21}(H_3)$ ,  $R_{H21}(H_3)$ , and  $\rho_{11}$  is the inaccuracy in the measurement of the dimensions of the sample; the errors on  $N_{21}(H_3)$  and  $R_{H21}(H_3)$  are on the order of 5%, while that on  $\rho_{11}$  is  $<10\%$ . The accuracy on the periods of the SdH oscillations is limited by the thermal smearing of the oscillations, and is on the order of 5% for the low-doped samples, but 10% for the highest-doped one, which had a lower mobility.

The SdH oscillations in  $\rho_{11}$  are shown in Fig. 1, and are periodic in  $1/H_3$ . Some peaks are visibly split in the raw traces, and the Fourier transforms of  $\rho_{11}(1/H_3)$  show two “frequencies” in  $1/\rho(1/H_3)$ , as shown in Table I. By comparison with the full calculated Landau level spectrum,<sup>19</sup> it was shown that the second frequency is a 2<sup>nd</sup> harmonic due to spin-splitting. The first period corresponds to a cross-sectional area of the Fermi surfaces also given in Table I. Following Fig. 7 in Ref. 12, we plot the hole densities measured by Hall effect as a function of the Fermi energy deduced from the measured areas of the Fermi surface in Table I using the UVB cyclotron masses.<sup>9</sup> We compare our results to those from the data of Refs. 9 and 12. Kohler<sup>9</sup> uses this procedure and shows that there is a marked increase in carrier density when the Fermi level reaches  $20.5\text{ meV}$  below the UVB, which is the evidence for the existence of the LVB. The mass parameters for this band have not been determined

TABLE I. Tin concentrations ( $x$ ) and magnetic field oscillation frequencies  $[\Delta(1/H)]^{-1}$  ( $T$ ) and the corresponding Fermi surface areas  $A_F$  for the three tested alloys.

$\text{Bi}_{2-x}\text{Sn}_x\text{Te}_3$	$[\Delta(1/H)]^{-1}$ ( $T$ )	$A_F$ ( $\text{m}^{-2}$ )
$x=0.0025$	12.15	$1.16 \times 10^{17}$
	24.2	
$x=0.0075$	11.3	$1.09 \times 10^{17}$
	22.3	
$x=0.015$	13.2	$1.25 \times 10^{17}$
	27.8	

as of yet, however, Kohler<sup>9</sup> indicates that the integral DOS mass of the LVB exceeds  $1.25m_e$ . Kulbachinskii<sup>11,13</sup> shows a second deviation in Sn doped  $\text{Bi}_2\text{Te}_3$  when the Fermi energy reaches  $15\text{ meV}$  below the top of the UVB. Here, taking the second frequency as a harmonic, we calculate Fermi level using the same procedure and our points fall in accordance with the points shown by Kulbachinskii.<sup>12</sup> We could mathematically arrive at a different conclusion if we assume that the second frequency corresponds to a second series of pockets on the Fermi surface,<sup>20</sup> which is not physical, but we lift this ambiguity with thermoelectric and thermomagnetic measurements.

The fundamental relation between the  $S$  and the carrier density  $p$  in each semiconductor band was called the “Pisarenko relation” by Ioffe.<sup>21</sup> It forms the reference with respect to which one establishes if one has successfully increased  $S$  for a given carrier concentration and scattering mechanism. The thermopower of degenerately doped  $\text{Bi}_2\text{Te}_3$  is isotropic and  $S_{11}$  equals the scalar partial hole coefficient  $S(p)$ .<sup>22</sup> We calculate the partial hole Seebeck coefficient  $S(p)$  for  $p$  type  $\text{Bi}_2\text{Te}_3$  as lines in Fig. 2, assuming that the relax-

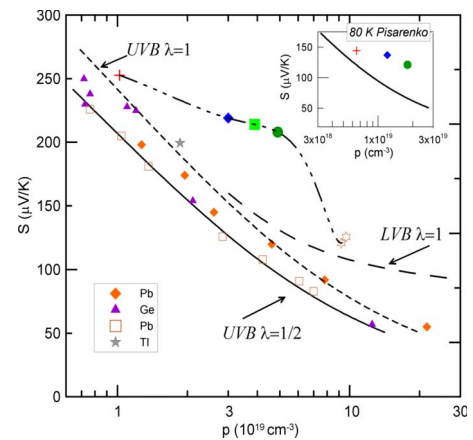


FIG. 2. (Color online) Pisarenko relation (solid and dashed line) for  $p$ -type  $\text{Bi}_2\text{Te}_3$  as calculated at  $300\text{ K}$ . The symbols are: (red plus)  $\text{Bi}_{1.9975}\text{Sn}_{0.0025}\text{Te}_3$ , (blue diamond)  $\text{Bi}_{1.9925}\text{Sn}_{0.0075}\text{Te}_3$ , (green dot)  $\text{Bi}_{1.985}\text{Sn}_{0.015}\text{Te}_3$ , (green square)  $\text{Bi}_{1.98}\text{Sn}_{0.02}\text{Te}_3$ , and (orange star)  $\text{Bi}_{1.95}\text{Sn}_{0.05}\text{Te}_3$ . The symbols for  $\text{Bi}_2\text{Te}_3$  doped with Pb (Refs. 23 and 24), Ge (Ref. 23), and Tl (Ref. 25) are shown in the figure. The inset contains the calculated Pisarenko relation at  $80\text{ K}$  as well as experimental points for  $\text{Bi}_{2-x}\text{Sn}_x\text{Te}_3$  as measured in this work.

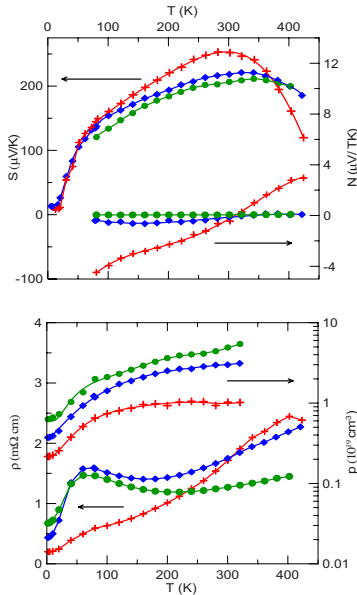


FIG. 3. (Color online) Resistivity  $\rho$ , carrier density  $p$ , Seebeck ( $S$ ), and isothermal transverse Nernst-Ettingshausen ( $N$ ) coefficients versus temperature. The points indicate the measured data, while the lines are added to guide the eye. The symbols are: (red plus)  $\text{Bi}_{1.9975}\text{Sn}_{0.0025}\text{Te}_3$ , (blue diamond)  $\text{Bi}_{1.9925}\text{Sn}_{0.0075}\text{Te}_3$ , and (green dot)  $\text{Bi}_{1.985}\text{Sn}_{0.015}\text{Te}_3$ .

ation time follows a power law of energy  $\tau = \tau_0 E^\lambda$ , where  $\lambda$  is the scattering exponent.<sup>18</sup> We calculate  $S(p)$  for two scattering mechanisms, optical scattering ( $\lambda=0.5$ ) and ionized impurity scattering, ( $\lambda=1$ ) at 300 and 80 K (inset) using an integral density of states effective mass of  $m_d^* = 0.35m_e$  of the UVB. We add an estimate of the influence of the LVB as a dashed line calculated with  $\lambda=1$  and  $m_{d,\text{LVB}}^* = 1m_e$ ; this is quite inaccurate, because the effective mass of the LVB is not well known,<sup>9</sup> and also because the temperature dependence of the band structure is not known and was not taken into account. We include literature data taken on  $p$ -type  $\text{Bi}_2\text{Te}_3$  (Refs. 23–25) at 300 K. The data follow trace for the UVB and ignore the effect of the LVB; we speculate that the relative position of the two bands must have a temperature dependence that is not known to date, and that the LVB probably moved with increasing temperature to a lower energy level with respect to the top of the UVB at 300 K than Kohler’s<sup>9</sup> measurements at 4.2 K indicate. We see that the scattering exponent that best fits the Seebeck data changes from 0.5 to 1 with increasing carrier concentration, indicating a progressive change from optical to ionized impurity scattering as expected. Upon placing the data measured at 300 K on the present  $\text{Bi}_{2-x}\text{Te}_3\text{Sn}_x$  samples onto the Pisarenko relation Fig. 2, we note a marked departure from that of the other similarly doped samples: this indicates the presence of a resonant level. The  $x=0.015$  sample has a  $S$  double that of samples doped to similar hole concentrations without Sn. We include the calculated 80 K Pisarenko relation and our experimental data points; thus demonstrating an increase between 50% to 250% in  $S$  over that of similarly doped  $\text{Bi}_2\text{Te}_3$ .

Refer to Fig. 3 for the summary of the galvanomagnetic and thermomagnetic measurements; a quantitative analysis is

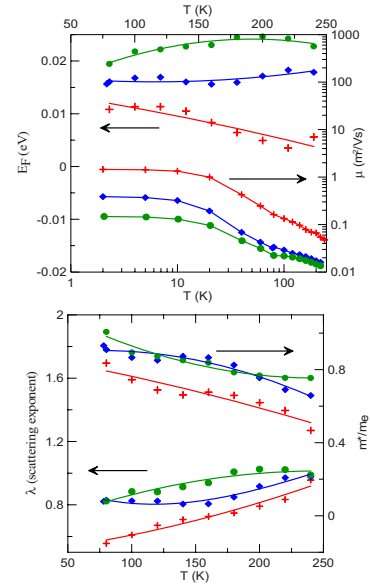


FIG. 4. (Color online) Summary of the four parameter fits using the degenerate equations. The symbols follow those in Fig. 3

given in the next paragraph. There is a sharp peak in electrical resistivity for both  $x=0.0075$  and  $x=0.015$  at 60 K. Below 300 K, when the samples are extrinsic, we show the Hall carrier density  $p = [q \cdot R_H]^{-1}$ , which increases with  $x$  and shows a sharp increase for  $20 \text{ K} < T < 120 \text{ K}$ . The thermopower  $S$  shows a large increase over a simple  $T^1$  law between 15–50 K. The Nernst coefficient  $N$  is the largest for  $x=0.0025$  and changes over temperature from negative ( $T \leq 250 \text{ K}$ ) to positive ( $T > 350 \text{ K}$ ), with its zero point crossing the temperature where  $S$  peaks. Both  $S$  and  $N$  show the onset of the effect of thermally excited electrons at  $T > 300 \text{ K}$ .<sup>21</sup>

At  $T \leq 250 \text{ K}$ , the samples are extrinsic and we use the measurements of four galvano- and thermomagnetic properties ( $\rho_{11}$ ,  $S_{11}$ ,  $N_{21}$ , and  $R_{H21}$ ) at each temperature to deduce four band structure parameters:<sup>17,18</sup> the hole density  $p$ , their mobility ( $\mu$ ), the Fermi energy  $E_F$  and/or the integral density of states effective mass  $m_d^*$ , and the scattering exponent  $\lambda$  defined above. The results of the four parameter fit are depicted in Fig. 4. We note that the Fermi levels of the two higher doped samples are “pinned” at approximately 15 and 20 meV, and that when extrapolated to 0 K,  $\lim_{T \rightarrow 0}(E_F) \approx 15 \text{ meV}$ , consistently with the results of the SdH measurements. The density of states effective mass  $m_d^*$  of the Sn-doped samples is approximately double that of the integral density of states mass of the UVB ( $0.35m_e$ ). This suggests the presence of an additional energy level distinct from the LVB, as the LVB has a much heavier mass yet ( $>1.25m_e$ ) (Ref. 9) and the calculated number of carriers if the second frequency is taken as real is 2–5 times more than that of the UVB. This confirms that the resonant level in Fig. 1 is real and that the second SdH frequency of 22–27 T is a harmonic, which appears in the Fourier transform of the SdH traces as a result of the spin splitting of the Landau levels. Electrical mobility drops with increasing hole concentration, and follows typical temperature dependence which is a mixture of ionized impurity scattering and optical phonon scattering.

The scattering exponent  $\lambda$  for the three samples is approximately  $0.7 \leq \lambda \leq 1$ , also indicating that the scattering mechanism is a mixture of ionized impurity and acoustic phonon scattering; this number is much less than the scattering exponent estimated<sup>26</sup> for scattering of charge carriers on the sharp excess DOS due to the Sn level and *a posteriori* justifies the assumptions made in calculating the Pisarenko relation.

Using an average dielectric constant of 73,<sup>27</sup> and the masses of Ref. 9, the Bohr radii of the UVB and LVB holes are 48 and 10 nm, respectively. The average distance between Sn atoms in our 3 samples being 4, 2.8, and 2.2 nm, respectively, we conclude that the Bohr radii overlap several Sn atoms.

In summary, we provide the first experimental evidence that Sn forms a resonant level in Bi<sub>2</sub>Te<sub>3</sub> that sufficiently distorts the density of states of the upper valence band to result in a strong increase in thermoelectric power. The thermoelectric power factors  $P=S^2\sigma$  of the single crystals in this

study are as follows. The  $x=0.0025\%$  sample has  $P > 45 \mu\text{W}/\text{cm K}^2$  from 170 to 300 K, the  $x=0.015$  sample has  $P > 33 \mu\text{W}/\text{cm K}^2$  for  $240 \text{ K} < T < 360 \text{ K}$ . The room-temperature in-plane power factor on these samples is considerably increased over that obtained on single-crystal samples of Scherer and Scherer<sup>28</sup> (range from 17 to  $27 \mu\text{W}/\text{cm K}^2$ ) which were doped *p* type with excess Bi to the same carrier concentrations. This is mainly due to the increase in Seebeck coefficient, while the mobility is not much decreased by the increase in effective mass at the Fermi energy. We point for completion out that there is a report in the literature that very high-quality single crystals<sup>29</sup> of Bi-rich of Bi<sub>2</sub>Te<sub>3</sub>, with room-temperature mobilities ( $800 \text{ cm}^2/\text{s}$ ) more than four times Scherer's or ours, display in-plane power factors actually equal to the ones reached here.

We acknowledge support by BSST, LLC.

- <sup>1</sup>J. P. Heremans *et al.*, *Science* **321**, 554 (2008).
- <sup>2</sup>J. Friedel, *Can. J. Phys.* **34**, 1190 (1956).
- <sup>3</sup>P. de Faget de Casteljau and J. Friedel, *J. Phys. Radium* **17**, 27 (1956); A. Blandin and J. Friedel, *ibid.* **20**, 160 (1959).
- <sup>4</sup>J. Kondo, *Prog. Theor. Phys.* **34**, 372 (1965).
- <sup>5</sup>B. A. Volkov *et al.*, *Phys. Usp.* **45**, 819 (2002).
- <sup>6</sup>V. I. Kaidanov *et al.*, *Sov. Phys. Semicond.* **26**, 113 (1992); Yu. I. Ravich, in *CRC Handbook on Thermoelectrics* edited by D. M. Rowe (CRC Press, Boca Raton, FL, 1995).
- <sup>7</sup>G. D. Mahan and J. O. Sofo, *Proc. Natl. Acad. Sci. U.S.A.* **93**, 7436 (1996).
- <sup>8</sup>V. Jovicic *et al.*, *J. Appl. Phys.* **103**, 053710 (2008).
- <sup>9</sup>H. Köhler, *Phys. Status Solidi B* **74**, 591 (1976).
- <sup>10</sup>*Physics of Non-Tetrahedrally Bonded Binary Compounds II*, edited by O. Madelung, Landolt-Bornstein, New Series, Group III, Vol. 17, Pt. f (Springer-Verlag, Berlin, 1983); the integrated density of states mass is the density of states mass of each pocket of the Fermi surface, multiplied by the number of pockets to the power 2/3.
- <sup>11</sup>V. A. Kulbachinskii *et al.*, *Phys. Status Solidi* **150**, 237 (1988).
- <sup>12</sup>V. A. Kulbachinskii *et al.*, *Phys. Rev. B* **50**, 16921 (1994).
- <sup>13</sup>V. A. Kulbachinskii *et al.*, *Phys. Status Solidi* **199**, 505 (1997).
- <sup>14</sup>M. K. Zhitinskaya *et al.*, Proceedings of the 16th International Conference on Thermoelectricity, IEEE 1997 (unpublished), p. 97.
- <sup>15</sup>M. K. Zhitinskaya *et al.*, *Phys. Solid State* **40**, 1297 (1998).
- <sup>16</sup>M. K. Zhitinskaya *et al.*, Proceedings of the European Thermoelectric Society Meeting, 2004 (unpublished) (<http://galaxy.uci.agh.edu.pl/~ets2004/proceedings/Zhitinskaya.PDF>) report measurements up to 400 K on Sn-doped Bi<sub>2</sub>Te<sub>3</sub> single crystals, but mention only "a modified temperature dependence of the transport coefficients," besides the presence of resonant states.
- <sup>17</sup>J. P. Heremans *et al.*, *J. Appl. Phys.* **98**, 063703 (2005).
- <sup>18</sup>J. P. Heremans *et al.*, *Phys. Rev. B* **70**, 115334 (2004).
- <sup>19</sup>N. Miyajima *et al.*, *J. Low Temp. Phys.* **123**, 219 (2001).
- <sup>20</sup>We could analyze the SdH results two ways: either the two oscillation frequencies arise from two different sets of degenerate sections of the Fermi surface, or the second frequency is a harmonic, and we just have one set of Fermi surface sections. Taking the second frequency as real, we calculate that it would correspond to cross-sections of the Fermi surface that are consistent with the LVB of Ref. 9. If we push this hypothesis further, we could use the Fermi level, total Hall carrier density, and SdH carrier density and effective mass of the UVB to deduce the density of carriers left in the LVB and their masses. The LVB hole density calculated under that hypothesis would be 2–5 times larger than that of the UVB, and the calculated LVB masses would approximately 1.5–3 $m_e$ , heavier than previously suggested.<sup>9</sup> Furthermore, the LVB masses would appear to depend on tin concentration. This mathematical possibility is unphysical because it contradicts the calculations based on the four transport parameters (Fermi level, effective mass, scattering exponent, and mobility), and because the second frequency can be assigned to spin splitting, Ref. 19.
- <sup>21</sup>A. F. Ioffe, *Physics of Semiconductors* (Academic, New York, 1960).
- <sup>22</sup>The Seebeck coefficient of Bi<sub>2</sub>Te<sub>3</sub> is anisotropic in general, but the partial Seebeck coefficients of each electron or hole pocket of the Fermi surface are scalars. The anisotropy arises from the fact that the total Seebeck coefficient is an average of the partial coefficients of each pocket weighted by the partial conductivities of those pockets, which are anisotropic.  $S_{11}$  is dominated by the partial hole Seebeck coefficient  $S$  in moderately *p*-type material.
- <sup>23</sup>G. Bergmann, *Z. Naturforsch.* **18a**, 1169 (1963).
- <sup>24</sup>T. Plecháček *et al.*, *Philos. Mag.* **84**, 2217 (2004).
- <sup>25</sup>Measured by the authors.
- <sup>26</sup>S. J. Thiagarajan *et al.*, *Phys. Status Solidi (RRL)* **1**, 256 (2007).
- <sup>27</sup>W. Richter *et al.*, *Phys. Status Solidi* **84**, 619 (1977).
- <sup>28</sup>S. Scherer and H. Scherer, in *CRC handbook on Thermoelectricity*, edited by D. M. Rowe (CRC Press, Boca Raton, FL, 1995), Chap. 19, p. 211.
- <sup>29</sup>C. H. Champness and A. L. Kipling, *Can. J. Phys.* **44**, 769 (1966).
- <sup>30</sup>V. A. Kul'bachinskii *et al.*, *Vestn. Mosk. Univ., Ser. 3: Fiz., Astron.* **30**, 68 (1989).